HHS Public Access

Author manuscript

Clin Cancer Res. Author manuscript; available in PMC 2017 February 01.

Published in final edited form as:

Clin Cancer Res. 2016 February 1; 22(3): 725–733. doi:10.1158/1078-0432.CCR-15-2867-T.

Novel *MYBL1* gene rearrangements with recurrent *MYBL1-NFIB* fusions in salivary adenoid cystic carcinomas lacking t(6;9) translocations

Yoshitsugu Mitani[1,*], **Bin Liu**[2,*], **Pulivarthi H. Rao**[3], **Vishnupriya J Borra**[3], **Mark Zafereo**[4], **Randal S. Weber**[4], **Merrill Kies**[5], **Guillermina Lozano**[2], **P. Andrew Futreal**[6], **Carlos Caulin**[4], and **Adel K. El-Naggar**[1,4]

[1]Department of Pathology, The University of Texas MD Anderson Cancer Center, Houston, Texas.

[2]Department of Genetics, The University of Texas MD Anderson Cancer Center, Houston, Texas.

[3]Department of Pediatrics, Baylor College of Medicine, Houston, Texas.

[4]Department of Head & Neck Surgery, The University of Texas MD Anderson Cancer Center, Houston, Texas.

[5]Department of Thoracic/Head & Neck Medicine Oncology, The University of Texas MD Anderson Cancer Center, Houston, Texas.

[6]Department of Genomic Medicine, The University of Texas MD Anderson Cancer Center, Houston, Texas.

Abstract

Purpose—Adenoid cystic carcinoma (ACC) is an indolent salivary gland malignancy, characterized by t(6;9) translocations and *MYB-NFIB* gene fusions in approximately 50% of the tumors. The genetic alterations underlying t(6;9)-negative and t(6;9)-positive/*MYB-NFIB*-fusion negative ACC remain unknown. To uncover the genetic alterations in ACC lacking the canonical translocation and fusion transcript and identify new abnormalities in translocation positive tumors.

Experimental Design—We performed whole genome sequencing in 21 salivary ACCs and conducted targeted molecular analyses in a validation set (81 patients). Microarray gene expression data was also analyzed to explore the biological differences between fusion positive and negative tumors.

Results—We identified a novel *MYBL1-NFIB* gene fusion as a result of t(8;9) translocation and multiple rearrangements in the *MYBL1* gene in 35% of the t(6;9)-negative ACCs. All *MYBL1* alterations involved deletion of the C-terminal negative regulatory domain and were associated with high *MYBL1* expression. Reciprocal *MYB* and *MYBL1* expression was consistently found in

Corresponding Authors: Adel K. El-Naggar, Department of Pathology, Unit 85, The University of Texas MD Anderson Cancer Center, 1515 Holcombe Blvd., Houston, TX 77030. Phone: 713-792-3109; Fax: 713-792-5532; anaggar@mdanderson.org Or Carlos Caulin, Department of Head and Neck Surgery-Research, Unit 123, The University of Texas MD Anderson Cancer Center, 1515 Holcombe Boulevard, Houston, TX 77030-4009. Phone: 713-794-5603; Fax: 713-745-2234; ccaulin@mdanderson.org.

*Contributed equally to this work

Competing Interests: The authors declare no conflict of interest

ACCs. Additionally, 5'-*NFIB* fusions that did not involve *MYB*/*MYBL1* genes were identified in a subset of t(6;9)-positive/fusion-negative tumors. We also delineated distinct gene expression profiles in ACCs associated with the length of the *MYB* or *MYBL1* fusions, suggesting a biological importance of the C-terminal part of these fusions.

Conclusion—Our study defines new molecular subclasses of ACC characterized by *MYBL1* rearrangements and 5'-*NFIB* gene fusions.

Keywords

Salivary adenoid cystic carcinoma; MYBL1; NFIB; MYB; fusion gene

Introduction

Adenoid cystic carcinoma (ACC), the second most common salivary gland malignancy, is characterized by a remarkable morphologic heterogeneity and protracted clinical course (1–3). Approximately 50% of ACC patients experience recurrence and metastasis in 5 to 10 years, to which no effective therapy is available (4–6). Despite mounting efforts aimed to improve the management of ACC patients, no significant progress has been made.

Recent molecular genetic studies of ACC have demonstrated low mutation frequency (7, 8), with tumor specific t(6;9) translocations resulting in *MYB-NFIB* gene fusions and high MYB expression in over 50% of tumors (9–11). The genetic alterations associated with ACCs lacking t(6;9) remain unknown (11, 12). We posit that in depth genomic analysis of this subset of tumors will uncover potential driver events.

To achieve this goal, we investigated a large cohort of ACC patients with and without t(6;9) and the *MYB-NFIB* fusion using whole genome sequencing (WGS) and multiple conventional molecular techniques for in depth characterization of their genomic alterations.

Materials and Methods

Patient samples

Tumor specimens were harvested from primary tumors of patients who underwent surgical resection at The University of Texas MD Anderson Cancer Center (Houston, TX) between 1981 and 2011, reviewed by a head and neck pathologist, immediately frozen and stored at −80°C until used (Supplementary Table S1). The study was approved by the MD Anderson Cancer Center Institutional Review Board.

Whole genome sequencing (WGS)

Genomic DNA was extracted using the Gentra Puregene tissue kit (Qiagen) according to the manufacturer's protocols. WGS was performed by Complete Genomics (CG, Mountain View, California, USA) using ACC tumors and matching normal samples. This platform is based on the unchained combinatorial probe anchor ligation (cPAL) chemistry on arrays of self-assembling DNA nanoballs (DNBs) (13). Raw data was processed by CG using Cancer Pipeline 2.4. Reads were aligned to the reference genome (National Center for Biotechnology Information (NCBI) Build 37) and variants were called and scored using a

local de novo assembly approach. The Complete Genomics Cancer Pipeline 2.4 generated the somatic mutation call with the somatic score >= −10 (Supplementary Table S2). The visualization of circos plots was also generated based on the highConfidenceJunctions files by the pipeline.

Identification of Gene fusions

The Ingenuity Variant Analysis (IVA) software (QIAGEN) was used to retrieve the in-frame fusions with genomic annotations. Based on the “highConfidenceJunctions*.tsv” files and MasterVar files from CG, the IVA system aligns sequences of left and right junctions to the reference genome (Human NCBI Build 37). Strand sequences consistently matched and located on separate genes were recorded as gene fusion (Supplementary Table S3).

Validation of the *MYBL1-NFIB* fusion by RT-PCR

Total RNA was extracted with the RNeasy Universal Kit (Qiagen) and the first-strand cDNA was synthesized using 2μg of total RNA by oligo(dT) primer and the SuperScript III reverse transcriptase (Invitrogen) according to the manufacturer's instructions. Then, the cDNA was used to detect *MYBL1-NFIB* fusion transcripts by PCR, using specific primers (Supplementary Table S4) and KAPA2G Fast PCR Kits (KAPA Biosystems). PCR products were gel-purified and either sequenced directly or cloned into the pCR2.1 vector (Invitrogen). Sanger sequencing was performed using ABI PRISM 3130 Genetic Analyzer (Applied Biosystems) at the DNA sequencing core facility of MD Anderson Cancer Center.

Fluorescence in-situ hybridization (FISH)

FISH was performed on touch preparations of fresh ACCs tissues to screen for the t(8;9) translocation. *MYBL1* gene BAC clone (RP11-271O1) and the *NFIB* gene clones (RP11-54D21 and RP11-79B9) were labeled with spectrum red and spectrum green, respectively (Abbott Laboratories). Probes hybridization was performed according to previously published procedure (10). For scoring, 200 individual nuclei were counted in each case and positive fusion was scored when >3% of cells had yellow signal. Individual cells were captured and processed using the Quantitative Image Processing System (Applied Imaging).

Quantitative RT-PCR for MYBL1 expression

Quantitative RT-PCR using duplicate samples was performed using the Applied Biosystems 7900HT Real-Time PCR Systems (Applied Biosystems) with KAPA SYBR FAST kit (KAPA Biosystems). Primers corresponding to the N-terminal of MYBL1 were used for amplification of MYBL1 transcripts, and ACTB gene was used as internal control (Supplementary Table S4). MYBL1 expression was determined by the ΔCT method, and relative expression was calculated relative to MYBL1 expression of pooled normal salivary gland tissue (Clontech).

Western blotting

Protein lysates from fresh tumor tissues was extracted using RIPA buffer. Aliquots of 20 μg of protein were loaded on SDS-PAGE gels, transferred to nitrocellulose membranes and

probed with rabbit polyclonal anti-MYBL1 (HPA008791, Sigma-Aldrich), MYB (EP769Y, Abcam) and anti-ACTB (Sigma-Aldrich) antibodies.

Immunohistochemistry (IHC)

IHC was performed using the MYBL1 antibody (HPA008791, Sigma-Aldrich). Freshly processed 4 μm thick unstained sections of MYBL1 fusion positive and negative ACCs underwent incubation with primary antibody on Autostainer Link 48 (Dako) according to the manufacturer's instructions. Nuclear staining in tumor cells was scored as positive

3'Rapid amplification of cDNA ends (3'RACE)

2ug of total RNA was used to synthesize the first-strand cDNA using the 3'RACE adapter primer (Invitrogen) and the SuperScript III reverse transcriptase (Invitrogen), using *MYBL1*-specific primers (GSP), and nested PCR weas performed using KAPA HiFi PCR Kits (KAPA Biosystems) with touch-down protocol and 3'RACE universal primer (AUAP).

Expression array analysis

Illumina HumanHT-12 V4 BeadChips was utilized for the gene expression microarrays that have been deposited in Array Express (E-MTAB-1397) (8). The expression array data were processed by linear normalization and further subjected to the differential analysis with the "limma" Bioconductor package (14). Gene Set Enrichment Analysis (GSEA) was downloaded from the website (http://www.broadinstitute.org/gsea/index.jsp) (15). *MYB* and *MYBL1* fusion description is mentioned in Supplementary Table S5.

Results

Whole genome sequencing analysis of ACC

To identify genomic alterations in ACCs lacking the t(6:9) translocation and in t(6;9) positive/fusion negative tumors, we performed WGS on a set of 21 fresh frozen tumors and matched normal tissue specimens (Supplementary Table S1). This test set comprised of nine t(6;9)-positive tumors, six of which had *MYB-NFIB* fusion transcripts, and 12 t(6;9)-negative tumors. WGS confirmed the presence of *MYB-NFIB* fusions in all six previously reported tumors (10, 11). In addition, this analysis revealed the presence of numerous gene fusions in 20 of the 21 tumors sequenced (Supplementary Table S3).

Remarkably, rearrangements of the *MYBL1* gene were found in 5 of the 12 t(6;9) negative tumors. These comprised of 4 tumors with *MYBL1-NFIB* fusions and one tumor with an intra-chromosomal rearrangement resulting in the fusion of the *MYBL1* and *YTHDF3* genes (Fig. 1A and B, Supplementary Fig. S1 and Supplementary Table S3). The breakpoints in the four tumors with *MYBL1-NFIB* fusions were located in introns 8 and 14 of the *MYBL1* gene and in intron 10 of the *NFIB* gene. Accordingly, only the last two exons of *NFIB* were part of the gene fusions.

Additionally, three of the t(6:9)-positive/*MYB-NFIB* transcript-negative tumors were found to have the 5' end of the *NFIB* gene fused to different gene partners (non-*MYB/MYBL1*

related), including *XRCC4*, *NKAIN2*, *PTPRD* and *AIG1* (Fig. 1B and Supplementary Table S3; see detailed information below).

In addition to the chromosomal rearrangements, mutational screening identified low rates of somatic mutations in this tumor sets (Supplementary Table S2) (7, 8). Of those, only one gene (*CREBP*) was found to be shared by tumors with *MYB-NFIB* fusions and the non-fusion group. Exclusive mutations were limited few genes and included *MUC12* and TFAP4 in *MYB* fusion group and *MAP10* and *OTOP* in the *MYBL1* fusion group. Interestingly, *NOTCH1* and *SPEN* mutations were identified in tumors with no *MYB* or *MYBL1* fusions, suggesting that the *NOTCH* pathway may be preferentially enriched in this group (Supplementary Fig. S2).

Analysis of *MYBL1-NFIB* and *MYBL1-YTHDF3* gene fusions in ACCs

The finding of *MYBL1* rearrangements in five of 12 t(6;9)-negative tumors and its structural similarity to the *MYB* gene (16, 17) led us to conduct in-depth analyses of *MYBL1-NFIB* and *MYBL1-YTHDF3* fusions. To confirm *MYBL1* rearrangements identified by WGS, we used a panel of primers designed to detect these alterations by RT-PCR (Supplementary Fig. S3A and Supplementary Table S4). The presence of *MYBL1-NFIB* fusion transcripts was confirmed in all four tumors identified by WGS (Fig. 1C and Supplementary Fig. S3B). Additionally, Sanger sequencing of the *MYBL1-NFIB* transcripts showed that exon 8 of *MYBL1* to be fused with either exon 11 or exon 12 of the *NFIB* gene in the two tumors in which the *MYBL1* breakpoint had been localized to intron 8 by WGS (AC10 and AC11, Fig. 1C and Supplementary Fig. S4). In the other two tumors (AC12 and AC13), where WGS identified the breakpoints in *MYBL1* intron 14, RT-PCR and Sanger sequencing showed *MYBL1* exons 14 or 15 to be fused with exon 11 and/or 12 of the *NFIB* gene (Fig. 1C and Supplementary Fig. S4).

Notably, we found that part of *NFIB* exon 12 was transcribed in alternative reading frame in the presence of *NEIB* exon 11, resulting in distinct amino acid sequences (Supplementary Fig. S4). The expression of multiple fusion transcripts in the same tumor with different exons of *MYBL1* or *NFIB* supports alternative splicing mechanism. FISH analysis using *MYBL1* and *NFIB* BAC clones confirmed the presence of t(8;9) translocations in all 4 tumors in which *MYBL1-NFIB* fusions were initially identified by WGS (Fig. 1D). We also confirmed the *MYBL1-YTHDF3* fusion in AC14 and detected this fusion in another tumor (AC15, Fig. 1C and Supplementary Fig. S5).

Validation analysis of the *MYBL1* rearrangement (81 tumors)

To assess the prevalence of *MYBL1* alterations, we analyzed a validation set of 81 ACCs comprised of 45 positive tumors for the t(6;9) translocation and 36 t(6;9)-negative tumors (10, 11). FISH analysis identified the t(8;9) translocation in 10 (27.8%) of the 36 t(6;9)-negative tumors; eight of these ACCs also had *MYBL1-NFIB* fusions (Table 1), where, *MYBL1* exons 8, 9, 14 or 15 were found fused to exon 11 or 12 of the *NFIB* gene. Thus, all the fusions involving the *MYBL1* gene had an intact DNA binding and transactivation domains and a disrupted C-terminal negative regulatory domain (Fig. 1E). No *MYBL1-YTHDF3* fusion was identified in any of the tumors in the validation set.

Expression of *MYBL1* transcript in ACCs with *MYBL1* rearrangements

To evaluate the mRNA expression of *MYBL1* in ACCs, we performed quantitative RT-PCR on all 102 ACCs (21 in the test set and 81 in the validation set). Remarkably, we observed high levels of *MYBL1* mRNA in all 12 tumors with *MYBL1-NFIB* fusions and in the two tumors with *MYBL1-YTHDF3* fusions (Fig. 2A). Surprisingly, we noted high *MYBL1* expression in three tumors lacking both *MYBL1* fusions and t(6;9)/t(8;9) translocations. To explore additional genomic events associated with *MYBL1* overexpression in these three tumors, we performed 3'RACE using specific primers for *MYBL1* (Supplementary Figs. S3A and S6A) and found *MYBL1* gene truncation at exons 9 or 10 in all three tumors (Table 1). In one tumor (AC79), *MYBL1* exon 10 was placed next to an intergenic sequence of chromosome 8, resulting in a truncated *MYBL1* transcript with nine additional coding nucleotides (Fig. 2B). In the second tumor (AC78), a *MYBL1* truncation occurred as a result of an inter-chromosomal translocation between exon 9 of *MYBL1* and intron 5 of the *RAD51B* gene (chromosome 14) (Supplementary Fig. S6B). In the third tumor (AC77), a *MYBL1* variant containing 15bp of intron 9 resulted in the generation of a premature termination codon (Supplementary Fig. S6B). A similar finding has previously been observed in pediatric low-grade gliomas (18).

Interestingly, we observed an inverse relationship between *MYB* and *MYBL1* expression in ACCs. The majority of the t(6:9) positive tumors, expressed high *MYB* and low *MYBL1* mRNA levels (Fig. 2A). Conversely, tumors with *MYBL1* gene rearrangements expressed high *MYBL1* and low *MYB* mRNA levels The small subset of ACCs that lacked both of the t(6;9) and t(8;9) translocations and *MYB* or *MYBL1* rearrangements expressed variable levels of *MYB* mRNA.

MYBL1 protein expression was assessed by Western blotting using a specific antibody against the C-terminal domain of MYBL1. Since the antibody recognized only *MYBL1* variants with intact exon 10, this analysis is relevant to tumors with *MYBL1* exon 14/15 fusions. We observed high MYBL1 protein expression in the 3 ACCs with *MYBL1* exon14/15 - *NFIB* exon11 gene fusions (Fig. 2C), but not in tumors with other *MYBL1* rearrangements. On the other hand, MYB protein was not detected in tumors with *MYBL1-NFIB* fusions. To assess the cellular localization of MYBL1 protein, we performed immunohistochemical staining using the same MYBL1 antibody. This analysis revealed robust nuclear staining for MYBL1 in myoepithelial cells in all ACCs with *MYBL1* alterations at exons 14 or 15, but not in tumors lacking *MYBL1* rearrangements (Fig. 2D). Normal salivary gland including the ductal and acinar elements was uniformly negative.

Expression profiling of *MYB-NFIB* and *MYBL1-NFIB* in ACCs

To explore global gene expression associated with *MYB-NFIB* and *MYBL1-NFIB* fusions in ACCs we analyzed microarray data previously generated in this study (Supplementary Table S5) (8). Differential expression analysis comparing 13 tumors with *MYB* or *MYBL1* fusions to 6 tumors lacking *MYB* or *MYBL1* fusions showed no significant changes in gene expression. Further GSEA analysis of the *MYB/MYBL1* fusion and non-fusion tumors showed that 126 genes sets enriched in non-fusion group (Supplementary Table S6, listed top highest 37 gene sets), whereas no differential gene set was enriched in the *MYB/MYBL1*

fusions group. Of note the 6 tumors lacking *MYB* or *MYBL1* fusions used in this analysis expressed high levels of *MYB*.

Interestingly, unsupervised clustering analysis of the 13 tumors with *MYB* or *MYBL1* fusions revealed that tumors with fusions that occurred after exon 11 of *MYB* or *MYBL1* ("long fusions") clustered together and away from tumors with fusions at exons 8 or 9 ("short fusions") (Fig. 2E, upper panel). Although supervised analysis found no significant expression differences between "long" and "short" fusions, GSEA analysis identified 19 gene sets significantly enriched in "long fusion", and 5 gene sets enriched in "short fusion" group (Supplementary Table S6). It is interesting to note that most of the gene sets enriched in the "long fusion" samples are related to RNA processing and regulation of translation (Fig. 2E lower panel), while gene sets related to tissue development were enriched in short fusions (Supplementary Table S6). These results suggest that the *MYB* and *MYBL1* fusions may share common biological functions based the length of the fusion products.

Gene fusions involving the 5' end of the *NFIB* gene

As noted above, WGS identified fusions of the 5'*NFIB* region, including exons 1 and 2, with no-*MYB* or *MYBL1* gene partners in three of the t(6;9)-positive tumors lacking *MYB-NFIB* gene fusions(Fig. 3A). In one tumor (AC09), we confirmed the fusion of *NFIB* exon 2 to *XRCC4* exon 4 as a result of t(5;9) (Fig. 3B). This tumor also had a translocation that fused *NFIB* intron 3 to an intergenic region located approximately 1Mb upstream of *MYB* (position 134,485,793 in chromosome 6). A second tumor (AC08) contained complex rearrangements of chromosomes 6 and 9 that resulted in fusion of *NFIB* exon 2 to *PTPRD* and *NKAIN2* genes (Supplementary Fig. S7A). However, we were unable to detect fusion transcripts by RT-PCR in this tumor. Of note, the *NKAIN2* gene was translocated to approximately 10Mb upstream of the *MYB* gene. The third tumor (AC07), with *NFIB-AIG1* gene fusion (Supplementary Figure S7B), has previously been confirmed (11). This tumor also had translocation of *NFIB* to a genomic region located approximately 0.1Mb upstream of the *MYB* gene.

In summary, we identified 12 tumors with *MYBL1-NFIB* fusions in a total of 102 ACCs (12%), representing 25% (12/48) of all t(6;9)-negative cases. *MYBL1* truncations were found in three cases and *MYBL1-YTHDF3* fusion was only detected in two cases in the entire cohort. Three tumors were found to have fusions of the 5'end of the *NFIB* gene with *XRCC4, NKAIN2, PTPRD* and *AIG1* genes (Fig. 3C).

Clinicopathologic correlations with *MYB* and *MYBL1* alterations

Clinicopathologic correlations with the molecular findings of the entire cohort showed only significant association between *MYB* alterations and recurrence and metastasis ($P = 0.042$, Supplementary Table S7). Kaplan-Meier analysis also showed a shorter survival for patients with *MYB* alterations compared to that of patients with *MYBL1* alterations ($P = 0.010$, log-rank test, Supplementary Fig. S8).

Discussion

We identified novel inter- and intra-chromosomal rearrangements of the *MYBL1* gene in 35% of t(6;9)-negative ACCs. These alterations comprised *MYBL1-NFIB* fusions as a result of chromosomal translocations of 8q13 and 9p23 regions, intra-chromosomal rearrangements leading to *MYBL1-YTHDF3* fusions and *MYBL1* truncations. These findings, together with our previously reported *MYB* gene rearrangements, highlight the unprecedented occurrence of two distinct chromosomal translocations involving two of the *MYB* gene family members in a mutually exclusive and tumor specific manner. We contend that the lack of these gene rearrangements in other salivary gland malignancies studied (data not shown) suggests that t(6;9) and t(8;9) translocations occur at spatially adjacent domains in ACC progenitor cell facilitating the homologous recombination during cell division in ACC (19).

Interestingly, all *MYB/MYBL1* fusions and truncations retained the DNA binding and the transactivation domains, suggesting an important role for these *MYB/MYBL1* variants in regulating gene expression and biological functions in ACC tumorigenesis. In addition, we observed that the breakpoints in these fusions resulted in the truncation of the C-terminal negative regulatory domain, a mechanism that has been linked to the activation of *MYB* family members (17, 20–22). The presence of *MYBL1-NFIB* fusions in ACCs has been confirmed in an independent study (23). However, the finding of *MYB* full length expression in some tumor suggests that loss of the C-terminal domain may not be an absolute requirement in the regulation of these genes in ACC. Our *MYBL1* gene rearrangements findings, however, are at variance with studies of pediatric gliomas where duplications and/or amplification of *MYBL1* are the main findings, and suggest that tissue specificity play a role (18, 24).

Our gene expression results show a mutually exclusive relationship between *MYB* and *MYBL1* alterations in most of tumors in our cohort. Only two tumors with t(8;9) translocation but negative *MYBL1-NFIB* fusion had low *MYBL1* and high *MYB* mRNA expression. The underlying event associated with the expressions of these genes is currently unknown. The results, however, suggest that both genes coordinately involved in ACC tumorigenesis. This is supported by evidence that *MYB* and *MYBL1* regulate the expression of common and specific set of genes (16), and by our current expression analysis and those of others (7, 25, 26). Interestingly, the finding of distinct differential gene profiles between “long” and “short” fusions of both genes and their association to RNA processing and translation highlights a potential biological importance of the C-terminal part of these fusions.

Further analysis of somatic mutations of the WGS data identified limited number of genes with alterations in ACC. Comparative mutational analysis of tumors based on the structural abnormalities of each group showed mutations in *MAP10* and *OTOF* in MYBL1 fusion group and mutations of *MUC12* and *TFAP4* genes in *MYB* alterations group. The oncogenic role and the clinical significance of these mutations will be investigated upon the validation if these mutations in larger cohort. Interestingly, we found that tumors lacking *MYB/MYBL1* alterations had mutations in *NOTCH1*, *SPEN*, and *MUC16*, genes that have been previously

reported to be mutated in ACC (7, 8), and lend further support to a potential role in ACC development. These findings suggest that different genetic events may underlie non-fusion derived ACC. In this context, alterations of the *NOTCH* pathway would characterize preferentially non-*MYB/MYBL1* tumors, while different mutations are linked to fusion-positive tumors. These findings, if validated, may allow for the substratification of patients for targeted therapy, especially with small molecule therapy for *NOTCH1*.

We also underscore a potential driver role of NFIB gene in a subset of ACC. In three t(6;9) positive/ MYB fusion negative tumors, the 5' end of *NFIB* was fused to non-*MYB*/*MYBL1* related genes. Interestingly, all tumors with 5'*NFIB* fusions had genomic segments translocated to upstream of the *MYB* gene and expressed high MYB, suggesting that placement of genomic segment in proximity to the *MYB* gene play a functional role in enhancing activation. Interestingly, all three tumors with these alterations occurred in male patients in their early forties and had distant metastatic disease.

Our clinicopathologic correlations showed an association between *MYB* alterations and poor patients' outcome in contrast to those with *MYBL1* alterations. Although these results may appear to conflict with the concept of coordinate functional relationship between *MYB* and *MYBL1*, the aggressive nature of *MYB* associated tumors could be attributed to other factors including enhanced genomic instability and/or epigenetic alterations with MYB associated tumors.

In summary, this study identifies distinct molecular subclasses of ACC, characterized by translocation of 8q and 9p and alterations and high expression of the *MYB* homologue, *MYBL1*, in tumors negative for t(6;9) that also lack MYB expression. These findings advance efforts to identify common biological pathways in ACC.

Supplementary Material

Refer to Web version on PubMed Central for supplementary material.

Acknowledgments

The authors thank Yan Cai, Deborah A. Rodriguez, and Cynthia F.Steward for material retrieval and follow-up information, Glenda M. Pullom for her secretarial and administrative assistance.

Funding: The study is supported in part by the NIH National Institute of Dental and Craniofacial Research and the NIH Office of Rare Diseases Research grant number U01DE019765, the SGTB (Salivary Gland Biorepository, HHSN268200900039C 04), the Head and Neck SPORE Program grant number P50 CA097007, R21DE023656, The Kenneth D. Muller professorship, The Center for Genetics and Genomics and an NCI CA-16672 grant, and The Adenoid Cystic Carcinoma Research Foundation.

References

1. Chomette G, Auriol M, Tranbaloc P, Vaillant JM. Adenoid cystic carcinoma of minor salivary glands. Analysis of 86 cases. Clinico-pathological, histoenzymological and ultrastructural studies. Virchows Arch A Pathol Anat Histol. 1982; 395:289–301. [PubMed: 6287713]
2. Batsakis JG, Luna MA, el-Naggar A. Histopathologic grading of salivary gland neoplasms: III. Adenoid cystic carcinomas. Ann Otol Rhinol Laryngol. 1990; 99:1007–1009. [PubMed: 2173892]

3. Locati LD, Bossi P, Perrone F, Potepan P, Crippa F, Mariani L, et al. Cetuximab in recurrent and/or metastatic salivary gland carcinomas: A phase II study. Oral Oncol. 2009; 45:574–578. [PubMed: 18804410]
4. Seaver PR Jr, Kuehn PG. Adenoid cystic carcinoma of the salivary glands. A study of ninety-three cases. American journal of surgery. 1979; 137:449–455. [PubMed: 218469]
5. Fordice J, Kershaw C, El-Naggar A, Goepfert H. Adenoid cystic carcinoma of the head and neck: predictors of morbidity and mortality. Archives of otolaryngology--head & neck surgery. 1999; 125:149–152. [PubMed: 10037280]
6. Laurie SA, Licitra L. Systemic therapy in the palliative management of advanced salivary gland cancers. J Clin Oncol. 2006; 24:2673–2678. [PubMed: 16763282]
7. Ho AS, Kannan K, Roy DM, Morris LG, Ganly I, Katabi N, et al. The mutational landscape of adenoid cystic carcinoma. Nat Genet. 2013; 45:791–798. [PubMed: 23685749]
8. Stephens PJ, Davies HR, Mitani Y, Van Loo P, Shlien A, Tarpey PS, et al. Whole exome sequencing of adenoid cystic carcinoma. J Clin Invest. 2013; 123:2965–2968. [PubMed: 23778141]
9. Persson M, Andren Y, Mark J, Horlings HM, Persson F, Stenman G. Recurrent fusion of MYB and NFIB transcription factor genes in carcinomas of the breast and head and neck. Proc Natl Acad Sci U S A. 2009; 106:18740–18744. [PubMed: 19841262]
10. Mitani Y, Li J, Rao PH, Zhao YJ, Bell D, Lippman SM, et al. Comprehensive analysis of the MYB-NFIB gene fusion in salivary adenoid cystic carcinoma: Incidence, variability, and clinicopathologic significance. Clin Cancer Res. 2010; 16:4722–4731. [PubMed: 20702610]
11. Mitani Y, Rao PH, Futreal PA, Roberts DB, Stephens PJ, Zhao YJ, et al. Novel chromosomal rearrangements and break points at the t(6;9) in salivary adenoid cystic carcinoma: association with MYB-NFIB chimeric fusion, MYB expression, and clinical outcome. Clin Cancer Res. 2011; 17:7003–7014. [PubMed: 21976542]
12. West RB, Kong C, Clarke N, Gilks T, Lipsick JS, Cao H, et al. MYB expression and translocation in adenoid cystic carcinomas and other salivary gland tumors with clinicopathologic correlation. Am J Surg Pathol. 2011; 35:92–99. [PubMed: 21164292]
13. Drmanac R, Sparks AB, Callow MJ, Halpern AL, Burns NL, Kermani BG, et al. Human genome sequencing using unchained base reads on self-assembling DNA nanoarrays. Science. 2010; 327:78–81. [PubMed: 19892942]
14. Ritchie ME, Phipson B, Wu D, Hu Y, Law CW, Shi W, et al. limma powers differential expression analyses for RNA-sequencing and microarray studies. Nucleic Acids Res. 2015; 43:e47. [PubMed: 25605792]
15. Subramanian A, Tamayo P, Mootha VK, Mukherjee S, Ebert BL, Gillette MA, et al. Gene set enrichment analysis: a knowledge-based approach for interpreting genome-wide expression profiles. Proc Natl Acad Sci U S A. 2005; 102:15545–15550. [PubMed: 16199517]
16. Rushton JJ, Davis LM, Lei W, Mo X, Leutz A, Ness SA. Distinct changes in gene expression induced by A-Myb, B-Myb and c-Myb proteins. Oncogene. 2003; 22:308–313. [PubMed: 12527900]
17. Ness SA. Myb protein specificity: evidence of a context-specific transcription factor code. Blood Cells Mol Dis. 2003; 31:192–200. [PubMed: 12972026]
18. Ramkissoon LA, Horowitz PM, Craig JM, Ramkissoon SH, Rich BE, Schumacher SE, et al. Genomic analysis of diffuse pediatric low-grade gliomas identifies recurrent oncogenic truncating rearrangements in the transcription factor MYBL1. Proc Natl Acad Sci U S A. 2013; 110:8188–8193. [PubMed: 23633565]
19. Meaburn KJ, Misteli T, Soutoglou E. Spatial genome organization in the formation of chromosomal translocations. Semin Cancer Biol. 2007; 17:80–90. [PubMed: 17137790]
20. Dini PW, Eltman JT, Lipsick JS. Mutations in the DNA-binding and transcriptional activation domains of v-Myb cooperate in transformation. J Virol. 1995; 69:2515–2524. [PubMed: 7884901]
21. Gonda TJ, Buckmaster C, Ramsay RG. Activation of c-myb by carboxy-terminal truncation: relationship to transformation of murine haemopoietic cells in vitro. EMBO J. 1989; 8:1777–1783. [PubMed: 2670562]

22. Lei W, Rushton JJ, Davis LM, Liu F, Ness SA. Positive and negative determinants of target gene specificity in myb transcription factors. J Biol Chem. 2004; 279:29519–29527. [PubMed: 15105423]

23. Brayer KJ, Frerich CA, Kang H, Ness SA. Recurrent Fusions in MYB and MYBL1 Define a Common, Transcription Factor-Driven Oncogenic Pathway in Salivary Gland Adenoid Cystic Carcinoma. Cancer Discovery. 2015 Dec 2. [Epub ahead of print].

24. Zhang J, Wu G, Miller CP, Tatevossian RG, Dalton JD, Tang B, et al. Whole-genome sequencing identifies genetic alterations in pediatric low-grade gliomas. Nat Genet. 2013; 45:602–612. [PubMed: 23583981]

25. Gao R, Cao C, Zhang M, Lopez MC, Yan Y, Chen Z, et al. A unifying gene signature for adenoid cystic cancer identifies parallel MYB-dependent and MYB-independent therapeutic targets. Oncotarget. 2014; 5:12528–12542. [PubMed: 25587024]

26. Moskaluk CA, Baras AS, Mancuso SA, Fan H, Davidson RJ, Dirks DC, et al. Development and characterization of xenograft model systems for adenoid cystic carcinoma. Lab Invest. 2011; 91:1480–1490. [PubMed: 21709671]

Statement of Translational Relevance

We report novel recurrent *MYBL1-NFIB* gene fusions, *MYBL1* gene rearrangements, and MYBL1 overexpression in t(6;9)-negative ACCs, and 5'-*NFIB* gene fusions in a subset of t(6;9)-positive/*MYB-NFIB*-negative ACCs. These findings provide new insights into the complex genetics of ACC and expand the role of the *MYB* gene family members in ACC tumorigenesis, for future targeted therapies of ACC patients.

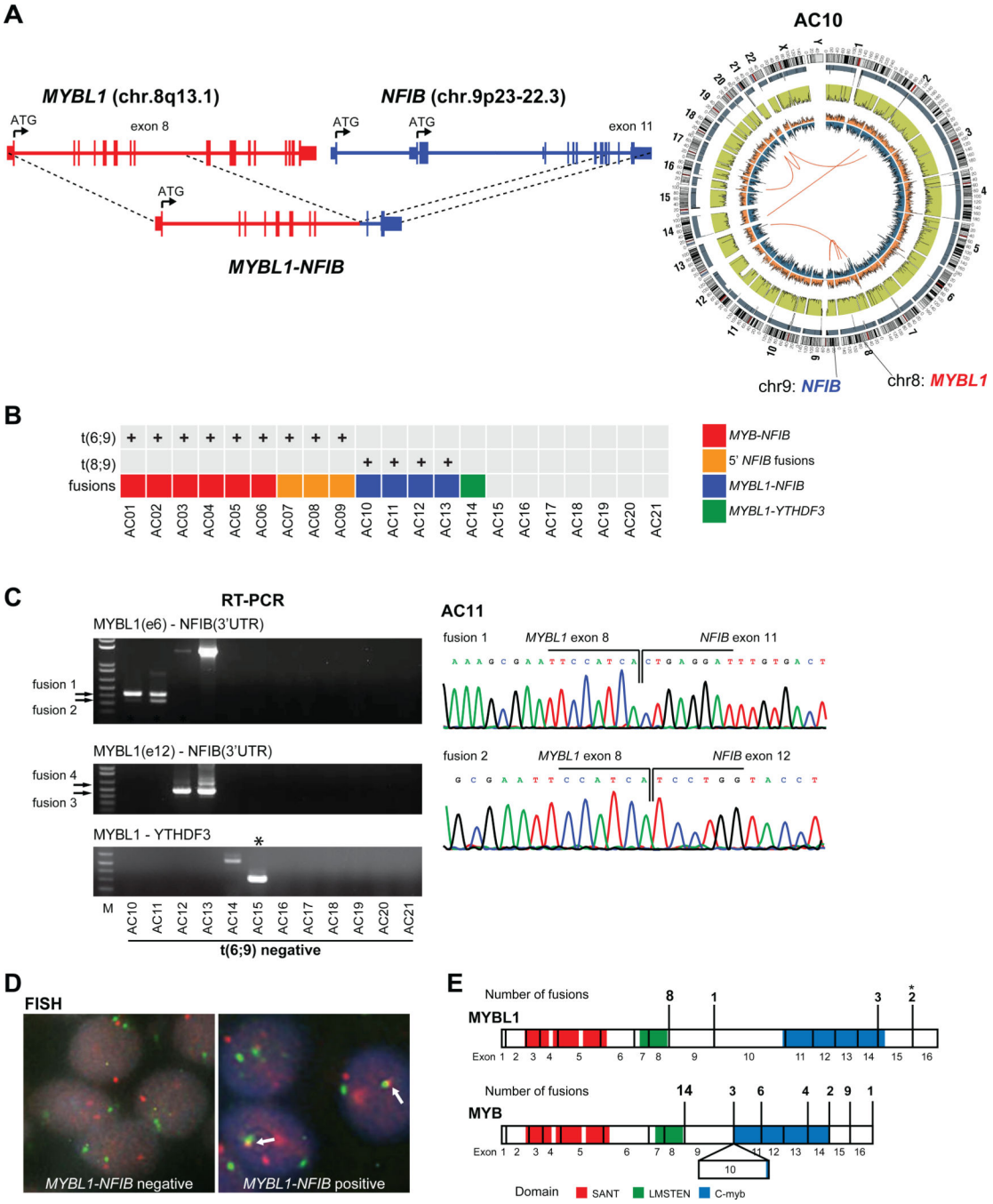

Figure 1. *MYBL1-NFIB* gene fusions identified in ACC lacking t(6;9) translocations

(A) Schematic outline of a representative example of *MYBL1-NFIB* gene fusion in t(6;9)-negative ACCs (left panel). In this case, exon 8 of *MYBL1* gene on chromosome 8 fused with exon 11 of the *NFIB* gene on chromosome 9. A circos plot illustrates global genomic rearrangements of the tumor containing this *MYBL1-NFIB* fusion (right panel); the chromosomal translocations identified by WGS are shown with orange lines. (B) Incidence of t(6;9) and t(8;9) translocations and associated *MYB-NFIB* (red) and *MYBL1-NFIB* (blue) fusions, in the 21 ACCs analyzed by WGS. The presence of the translocations was assessed

by FISH. The *MYBL1-YTHDF3* fusion (green) is also indicated. 5' *NFIB* fusions (orange) represent tumors in which the 5' end of *NFIB* was found fused to genes other than *MYBL1* or *MYB* (see Supplementary Table S3). (C) RT-PCR analysis for the detection of the *MYBL1-NFIB* and *MYBL1-YTHDF3* transcripts in t(6;9)-negative ACCs (left panel). Sanger sequencing confirmed the *MYBL1-NFIB* gene fusions (right panel). Note that two different fusion transcripts were identified in tumor AC11: *MYBL1* exon 8 linked to *NFIB* exon 11 (fusion 1) and exon 12 (fusion 2). (*) *MYBL1-YTHDF3* fusion was not identified by WGS in AC15. (D) FISH analysis using BAC clones containing *MYBL1* (red) and *NFIB* (green) genes. The yellow signals pointed by white arrow represent the *MYBL1* and *NFIB* gene fusion. (E) Schematic representation of the exon structure of the *MYBL1* and *MYB* genes showing the breakpoint locations in these genes in their fusions to *NFIB*. The number of cases with *MYBL1-NFIB* or *MYB-NFIB* fusions is listed above each gene and exon numbers are shown below the gene. (*) 2 tumors had two different *MYBL1* fusions each (see Table 1, tumors AC13 and AC73).

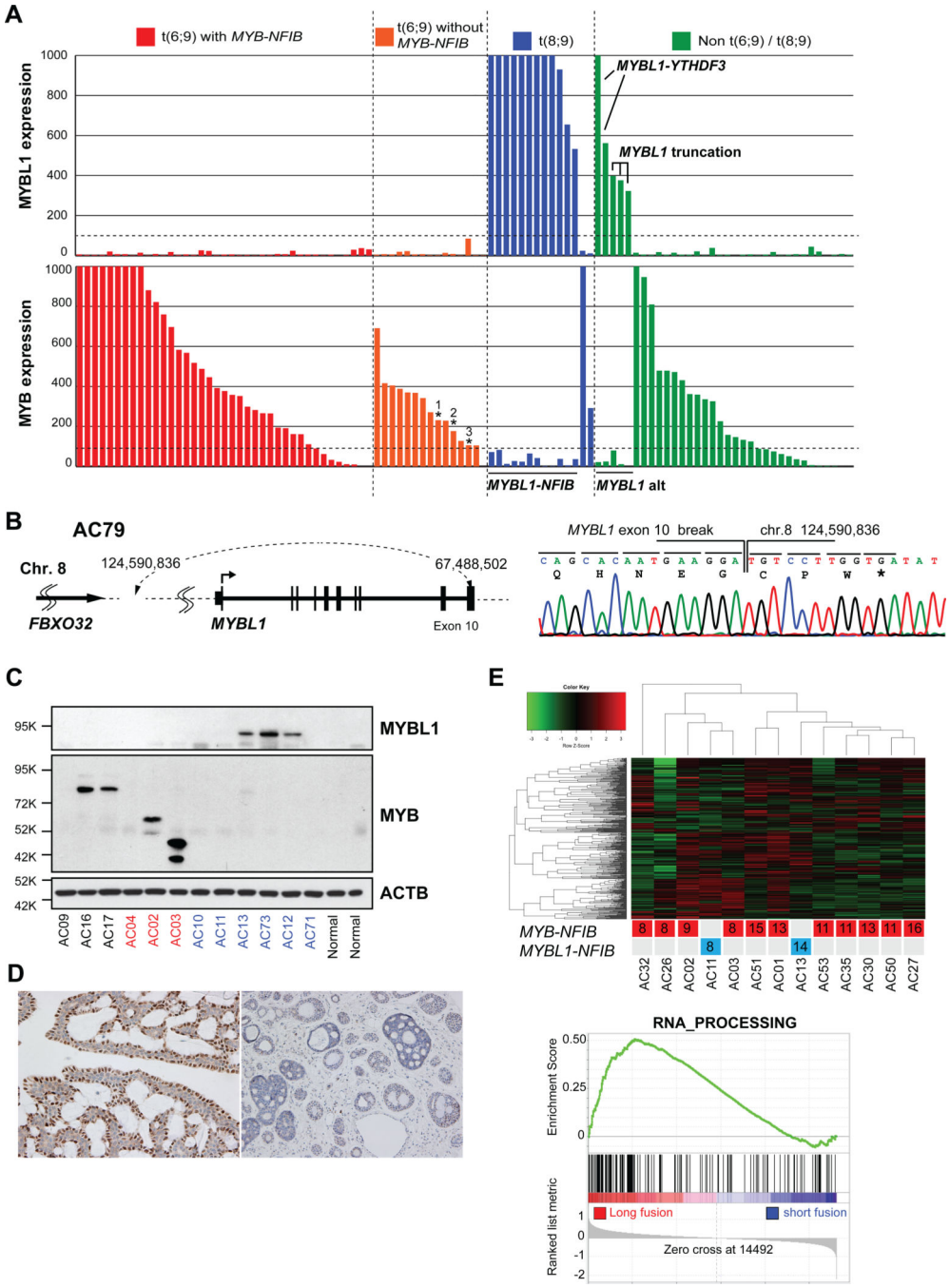

Figure 2. Mutually exclusive overexpression of *MYBL1* and *MYB* in ACCs

(A) Quantitative RT-PCR analysis for *MYB* and *MYLB1* mRNA expression performed on 102 ACCs. Tumors with t(6;9) translocation and *MYB-NFIB* fusion (red), t(6;9) without *MYB-NFIB* (orange), t(8;9) translocation (blue), and tumors lacking both t(6;9) and t(8;9) (green). Tumor samples in the top and bottom panels were aligned to visualize the expression of *MYBL1* (top panel) and *MYB* (bottom panel) in the same tumors. All of t(8;9) tumors but two had *MYBL1-NFIB* fusion; these two tumors had high MYB expression. Note that *MYBL1* alterations not involving *NFIB* (*MYBL1* alt) were found in a subset of tumors

lacking t(6;9) and t(8;9). Specifically, two tumors had a *MYBL1-YTHDF3* fusion and three tumors had *MYBL1* truncations, as indicated. *MYBL1* overexpression was found in all tumors with *MYBL1* rearrangements. Gene fusions involving the 5' end of *NFIB* were identified by WGS in 3 cases, indicated with (*): 1 (AC07), 2 (AC08) and 3 (AC09). (B) Schematic representation of a *MYBL1* truncation at exon 10 as a result of an intra-chromosomal translocation of chromosome 8. The sequencing profile for this truncation is shown on the right panel. (C) Western blotting analysis for MYBL1 expression in ACCs. Samples labeled in red or blue indicate *MYB-NFIB* or *MYBL1-NFIB* positive cases, respectively. Normal samples represent matched normal specimens for cases AC10 and AC11. Note that the MYBL1 antibody was raised against the C-terminal end of MYBL1, and only *MYBL1-NFIB* fusions with exon 14/15 of MYBL1 could be identified. Note that MYB was not detected in tumors carrying *MYBL1-NFIB* fusions. (D) Immunohistochemistry for MYBL1 showing nuclear staining in an ACC with *MYBL1-NFIB* fusion (left panel). MYBL1 was not detected in ACC tumor without MYBL1 alterations (right panel). (E) Unsupervised analysis of expression profiles of ACCs with different *MYB* and *MYBL1* alterations (upper panel). The numbers indicate the breakpoint exon for *MYB* or *MYBL1* in *MYB-NFIB* or *MYBL1-NFIB* fusions, respectively. Note that tumors with proximal and distal fusions tend to cluster together, respectively. The gene set enrichment analysis (GSEA) analysis indicates enrichment of RNA processing in "Long fusion", which were fusions that occurred after exon 11 of *MYB* or *MYBL1*. "Short fusion" comprised tumors with fusions at exons 8 or 9.

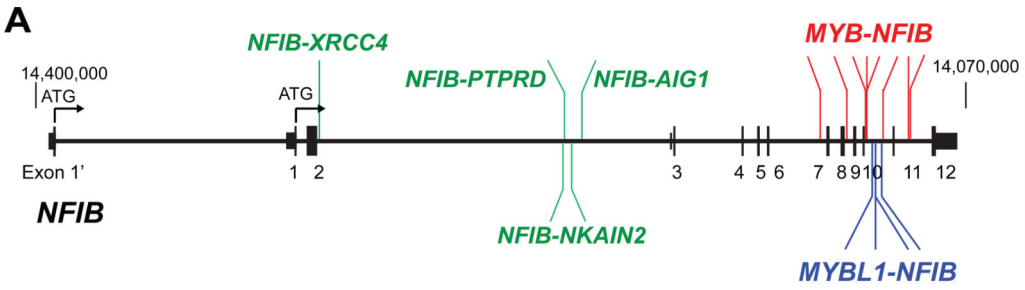

Sample ID	*NFIB* fused to		
	Chr	Position	Gene Name
AC09	5	82432698	*XRCC4*
AC08	6	124274111	*NKAIN2*
	6	124743630	*NKAIN2*
	9	9131303	*PTPRD*
AC07	6	143599306	*AIG1*

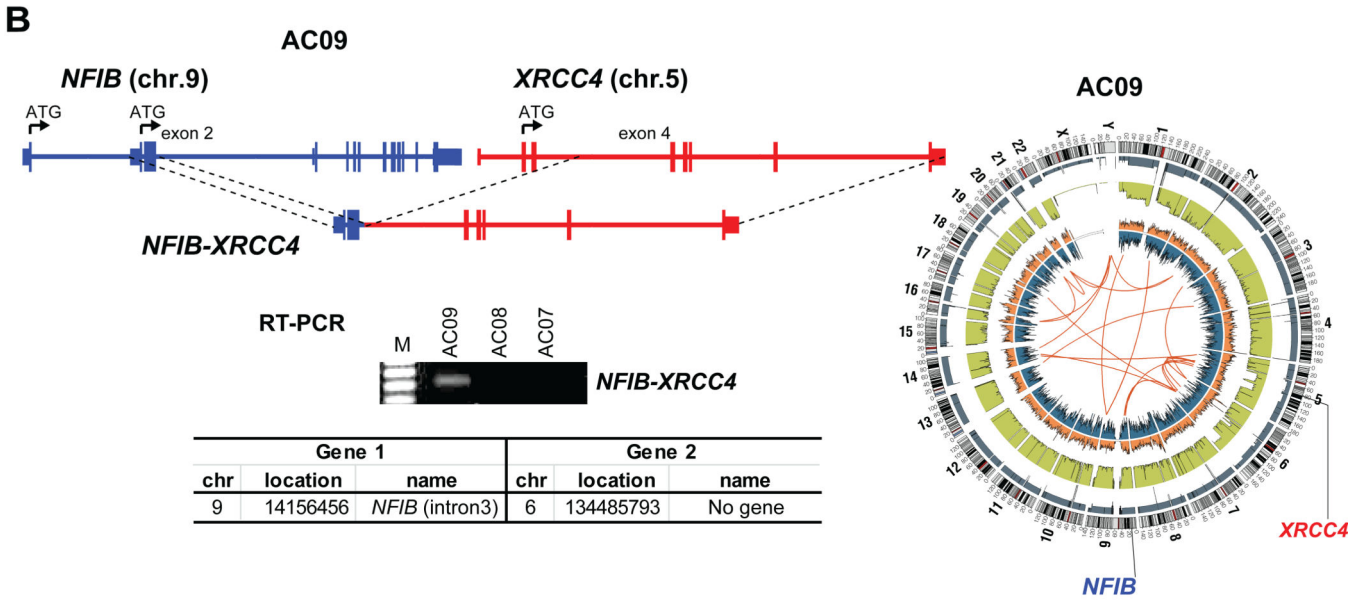

Gene 1			Gene 2		
chr	location	name	chr	location	name
9	14156456	*NFIB* (intron3)	6	134485793	No gene

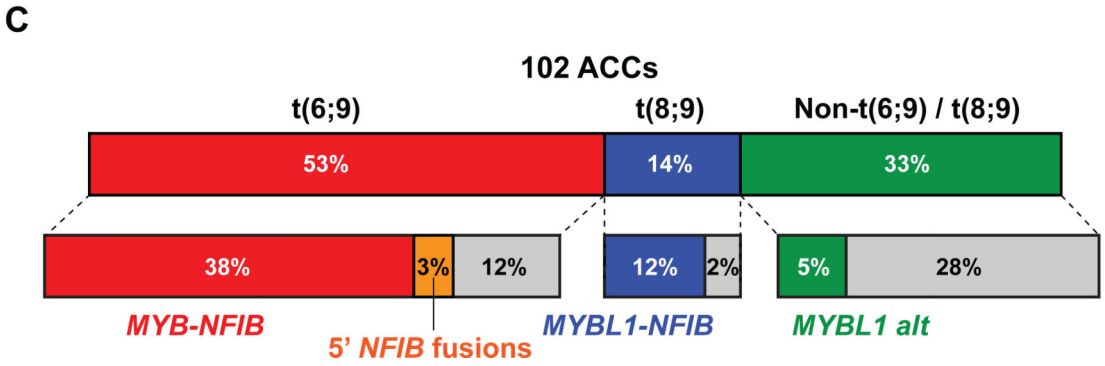

Figure 3. Analysis of *NFIB* gene fusions

(A) Location of *NFIB* gene breakpoints in *MYBL1-NFIB* and *MYB-NFIB* fusions and those in which the 5' end of *NFIB* is fused to *XRCC4*, *PTPRD*, *NKAIN2* and *AIG1*. Note that the breakpoints of *NFIB* in the *MYBL1-NFIB* fusions are clustered in intron 10, whereas those in *MYB-NFIB* fusions tend to be scattered across introns 6–10. All the breakpoints in the *NFIB* gene in 5' *NFIB* fusions were found in intron 2. Adjacent table lists all three cases with 5' *NFIB* fusions and the location of the breakpoints in fusion partners. (B) Schematic representation of the *NFIB-XRCC4* fusion depicting the 5'end of the *NFIB* gene in fusion with the 3' end of *XRCC4* (left panel). The corresponding circos plot for the tumor with this alteration is shown on the right panel; the chromosomal translocations identified by WGS

are shown with orange lines. The *NFIB-XRCC4* fusion transcript in AC09 was confirmed by RT-PCR. Tumors AC07 and AC08 were used a negative controls. (C) Summary of the frequency of t(6;9) and t(8;9) translocations and the associated *MYB-NFIB* and *MYBL1-NFIB* fusions and other *MYBL1* rearrangements (*MYBL1* alt) identified in the 102 ACCs analyzed in this study. The tumors comprised 53% with t(6;9), 14% with t(8;9) and 33% of tumors lacking both t(6;9) and t(8;9). The incidence of *MYB-NFIB* and *MYBL1-NFIB* fusions is indicated. Overall, *MYBL1* alterations were found in 17% of the tumors, 12% of them containing *MYBL1-NFIB* fusions and 5% of them (*MYBL1* alt) with *MYBL1* truncations or *MYBL1-YTHDF3* fusions.

Table 1

MYBL1 gene rearrangements in t(6;9)-negative ACC

Sample ID	t(8;9)[a]	*MYBL1* rearrangement
AC10	Positive	*MYBL1* exon8 - *NFIB* exon11
AC11	Positive	*MYBL1* exon8 - *NFIB* exon11 *MYBL1* exon8 - *NFIB* exon12
AC12	Positive	*MYBL1* exon14 - *NFIB* exon11
AC13	Positive	*MYBL1* exon14 - *NFIB* exon11 *MYBL1* exon15 - *NFIB* exon11
AC69	Positive	*MYBL1* exon8 - *NFIB* exon11
AC74	Positive	*MYBL1* exon8 - *NFIB* exon11 *MYBL1* exon8 - *NFIB* exon12
AC70	Positive	*MYBL1* exon8 - *NFIB* exon11 *MYBL1* exon8 - *NFIB* exon12
AC71	Positive	*MYBL1* exon9 - *NFIB* exon11
AC73	Positive	*MYBL1* exon14 - *NFIB* exon11 *MYBL1* exon15 - *NFIB* exon11
AC72	Positive	*MYBL1* exon8 - *NFIB* exon12
AC68	Positive	*MYBL1* exon8 - *NFIB* exon11 *MYBL1* exon8 - *NFIB* exon12
AC67	Positive	*MYBL1* exon8 - *NFIB* exon12
AC14	Negative	*MYBL1* exon9 - *YTHDF3* exon4
AC15	Negative	*MYBL1* exon8 - *YTHDF3* exon4
AC79	Negative	*MYBL1* truncation (*MYBL1* exon10 break)
AC78	Negative	*MYBL1* truncation (*MYBL1* exon9 - *RAD51B* intron 5)
AC77	Negative	*MYBL1* truncation (*MYBL1* exon9 - intron9)

[a] t(8;9) was determined by FISH.

MYBL1 alterations were confirmed by RT-PCR, Sanger sequencing, and 3'RACE.